Toward a Possibility To Exchange CO2 and CH4 in sI Clathrate Hydrates

ARTICLE *in* THE JOURNAL OF PHYSICAL CHEMISTRY B · FEBRUARY 2012

Impact Factor: 3.3 · DOI: 10.1021/jp2119586 · Source: PubMed

3 AUTHORS, INCLUDING:

Kirill Glavatskiy
University of Queensland
35 PUBLICATIONS **118** CITATIONS
SEE PROFILE

Signe Kjelstrup
Norwegian University of Science and Technol…
316 PUBLICATIONS **3,706** CITATIONS
SEE PROFILE

THE JOURNAL OF PHYSICAL CHEMISTRY B

Article

pubs.acs.org/JPCB

Toward a Possibility To Exchange CO_2 and CH_4 in sI Clathrate Hydrates

K. S. Glavatskiy,*[,†,‡] T. J. H. Vlugt,[‡] and S. Kjelstrup[†,‡]

[†]Department of Chemistry, Norwegian University of Science and Technology, NO 7491 Trondheim, Norway

[‡]Department of Process and Energy, Delft University of Technology, Leeghwaterstraat 44, 2628 CA Delft, The Netherlands

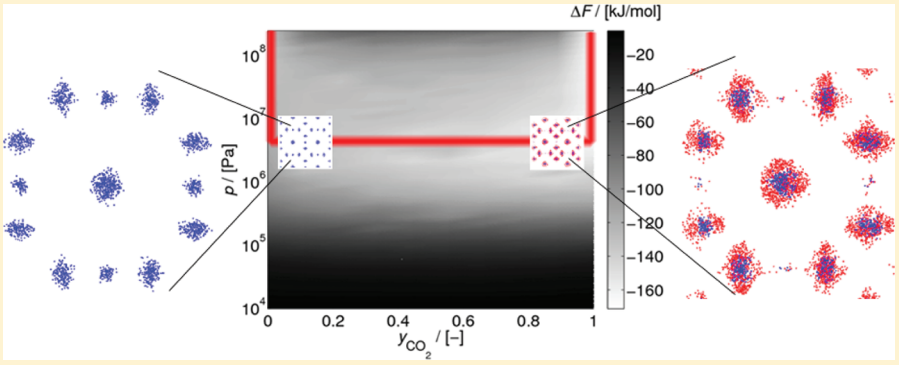

ABSTRACT: We study the thermodynamic conditions for exchange of CH_4 with CO_2 in sI clathrate hydrates using Grand Canonical Monte Carlo simulations. From the variations in the Helmholtz energy, we suggest a thermodynamic path for exchange of CH_4 by CO_2. The results can be understood from single-component occupancy isotherms. Simulations of pure component systems show that all methane sites are essentially equivalent, whereas carbon dioxide distinguishes between two types of sites, large or small. Mixture of CO_2 and CH_4 in the clathrate can be regarded as ideal, as long as only the large sites are occupied. A strong preference in selectivity is demonstrated for methane when the smaller sites become filled. The Helmholtz energies of the hydrate with a CO_2−CH_4 gas mixture for temperatures between 278 and 328 K and pressures between 10^4 and 10^9 Pa indicate that there exists a region of stability of a mixed hydrate referred to single-component hydrates.

1. INTRODUCTION

Understanding the possibility to exchange CH_4 with CO_2 in clathrate hydrates is of great importance to the oil industry and has been the focus of several studies.[1−5] By studying the radial distribution function of a fully occupied sI hydrate using molecular dynamic simulations, Geng et al.[6] recently suggested that a CO_2 + CH_4 mixture in the sI hydrate lattice can be more stable than a filled hydrate with pure components, CH_4 or CO_2. The present work aims to find the conditions for stability, using Grand Canonical Monte Carlo simulations (GCMC) of pure CO_2 and CH_4 as well as mixtures of CO_2 and CH_4 in an sI hydrate.

Monte Carlo simulations of this type are well-suited for this purpose because they allow one to study also metastable configurations, in particular, nonfully occupied hydrates.[7−9] Molecular simulations allow one to study the conditions of hydrate formation that are complicated to find experimentally. The quantities relevant for the formation process, namely, the change of the Gibbs or Helmholtz energy and the enthalpy due to the presence of one extra gas molecule in the hydrate, are easily calculated in GCMC simulations. For a particular configuration of a hydrate with encaged guest molecules, one can use the occupancy isotherms (the number of the gas molecules present in the cages as a function of their chemical potential) to obtain the Helmholtz energy, which can be used to give information about relative stabilities. We shall take advantage of the method development previously described for hydrates.[9,10]

Methane and carbon dioxide hydrates under typical reservoir conditions (for example, pressures up to 10^4 bar or 10^9 Pa, which corresponds to reservoir depths up to 10 km[2]) form sI clathrate structure. The structure, which is well-established,[11] has eight cages per unit cell. Interaction potentials for water are available from the literature.[12] We will use a rigid water model and the rigid framework model for all of the calculations. The typical behavior of the occupancy isotherms remains essentially unaltered when the hydrate framework model becomes flexible (and is therefore not presented here). For a rigid framework, the Helmholtz energy is relevant for the study of the system's stability, as the volume of the system remains constant.

The question of practical interest is when conditions favor hydrate formation from a gaseous of liquid mixture of water,

Received: December 12, 2011
Revised: February 24, 2012
Published: February 24, 2012

   dx.doi.org/10.1021/jp2119586 | J. Phys. Chem. B 2012, 116, 3745−3753

methane, and carbon dioxide. This can be written schematically as the reaction

$$[N_{CH_4} + N_{CO_2} + N_{H_2O}]_{\text{gas or liquid}} \rightleftharpoons [(N_{CH_4} + N_{CO_2})\cdot N_{H_2O}]_{\text{solid}} \quad (1)$$

Note that the process described by eq 1 is not a chemical reaction, as there are no changes in chemical bonding. It is useful to apply this notation to stress the importance of an energy barrier between the left- and right-hand sides of eq 1.

Depending on temperature/pressure, the reactants on the left-hand side of eq 1 are in either the gas or liquid phase. For a spontaneous process at constant volume and temperature, the change of the Helmholtz energy, that is, the energy of formation $\Delta_r F$, is negative. The long-term aim of the work is to obtain the values for $\Delta_r F$ that would decide whether the hydrate formation is favorable. To perform this task, we consider the above reaction as a two-stage process: (a) the formation of empty gas hydrate framework (a clathrate framework) from a gas or liquid and (b) the encapsulation of guest molecules of CO_2 or CH_4 into the cages of the clathrate

$$[N_{CH_4} + N_{CO_2} + N_{H_2O}]_{\text{gas or liquid}} \rightleftharpoons [N_{CH_4} + N_{CO_2}]_{\text{gas}} + [N_{H_2O}]_{\text{clathrate}} \quad (2a)$$

$$[N_{CH_4} + N_{CO_2}]_{\text{gas}} + [N_{H_2O}]_{\text{clathrate}} \rightleftharpoons [(N_{CH_4} + N_{CO_2})\cdot N_{H_2O}]_{\text{hydrate}} \quad (2b)$$

In this scheme, the empty hydrate can be seen as a hypothetical reference state thermodynamic calculations.[9,13] As the Helmholtz energy is a state function, the two processes can be studied independently and $\Delta_r F$ is then the sum of the Helmholtz energies of the two subprocesses.

In this Article, we focus on the second step of the hydrate formation, namely, we consider a clathrate framework and study the energetic effect of encapsulation of guest molecules into the empty cages of the hydrate. From a computational point of view, this process has many similarities to the adsorption of small molecules in porous materials such as zeolites and metal organic frameworks. GCMC simulations have been used extensively to study adsorption processes in zeolites and other porous materials.[14,15] In fact, the computational schemes as used in Monte Carlo simulation are identical for gas hydrates and zeolites, and we shall make use of this in this work.

In particular, we are interested in the change of the Helmholtz energy of the hydrate with a mixed gas encaged, $[(N_{CH_4} + N_{CO_2})\cdot N_{H_2O}]_{\text{hydrate}}$, compared with a metastable clathrate $[N_{H_2O}]_{\text{clathrate}}$ with N_{CH_4} and N_{CO_2} isolated molecules. This difference is denoted by ΔF in this Article and will be called the Helmholtz energy of encapsulation. Because adding a gas molecule in a cage stabilizes the hydrate, this Helmholtz energy of encapsulation will normally decrease with the loading. The quantities $\Delta_r F$ and ΔF are related, but we will return to the relationship and a discussion of $\Delta_r F$ in a subsequent paper. Furthermore, we are interested in the partial molar heat of encapsulation, which is the change of internal energy due to presence of an extra guest molecule in the hydrate. Both the Helmholtz energy of encapsulation and the heat of encapsulation are important for understanding the process of hydrate formation. The purpose of the Article is to discuss how these quantities can be understood in terms of molecular behavior and how the molecular behavior can help us design a path for exchange of methane by carbon dioxide.

The Article is organized as follows. In Section 2, we discuss the basic thermodynamic relations that allow us to calculate the Helmholtz energy and the so-called molar heat of encapsulation as a function of loading. The details of the simulations are specified in Section 3. In Section 4, we provide our results. We report occupancy isotherms for the single-component sI hydrates and the mixture of CO_2 and CH_4 in the sI hydrate as well as the selectivity data for the mixture hydrate. Furthermore, we calculate the Helmholtz energy difference ΔF of the above hydrates as a function of loading. Finally, we compare the data for the molar heat of encapsulation with the structure of the hydrates. Overall discussion and conclusion are given in Section 5.

2. THERMODYNAMICS

2.1. Helmholtz Energy. We consider the framework of water molecules in the sI clathrate structure. In simulations, we can control whether this framework is flexible or rigid. In both cases, we specify and keep fixed the lattice parameters of the framework, so the volume of the system V is constant. We also keep the temperature T of the system fixed.

The Helmholtz energy, F, of the clathrate with given numbers of encaged guest molecules (a loading) is given by[16]

$$F = -pV + \mu_w N_w + \sum_{i=1}^{n} \mu_i N_i \quad (3)$$

Here p is the pressure in the system, μ_i is the chemical potential of the ith guest component, and N_i is the number of encaged molecules of component i, whereas μ_w and N_w are the corresponding quantities for water. The number of guest compounds is n. For pure components, $n = 1$, for a mixture of methane and carbon dioxide, $n = 2$. The number of water molecules is fixed, whereas the number of guest molecules varies. The chemical potentials and therefore the Helmholtz energy depend on the loading.

We would like to calculate $\Delta F(N_{\{i\}}) \equiv F(N_{\{i\}}) - F(0)$, the difference in the Helmholtz energy of a filled clathrate $F(N_{\{i\}}) \equiv F(N_w,N_1,\cdots,N_n)$ and the Helmholtz energy of the empty clathrate $F(0) = F(N_w,0,...,0) = -pV + \mu_w N_w$. We refer to this difference as the Helmholtz energy of the mixture of gases in the hydrate. It follows from eq 3 that

$$\Delta F(N_{\{i\}}) = -[p(N_{\{i\}}) - p(0)]V + [\mu_w(N_{\{i\}}) - \mu_w(0)]N_w + \sum_{i=1}^{n} \mu_i(N_{\{i\}})N_i \quad (4)$$

where $p(N_{\{i\}})$ is the hydrostatic pressure at the given volume and loading, whereas $p(0)$ is the hydrostatic pressure at the same volume and zero loading. According to the Gibbs–Duhem relation, we have

$$SdT - Vdp + N_w d\mu_w + \sum_{i=1}^{n} N_i d\mu_i = 0 \quad (5)$$

dx.doi.org/10.1021/jp2119586 | J. Phys. Chem. B 2012, 116, 3745–3753

Integrating the equation at a constant temperature, volume, and a constant number of water molecules from zero loading to a given loading, we obtain

$$-V[p(N_{\{i\}}) - p(0)] + N_w[\mu_w(N_{\{i\}}) - \mu_w(0)] + \sum_{i=1}^{n} \int_{-\infty}^{\mu_i^*(N_{\{i\}})} N_i d\mu_i(N_{\{i\}}) = 0 \quad (6)$$

which, after substitution into eq 4 and integration by parts, gives[9]

$$\Delta F(N_{\{i\}}) = \sum_{i=1}^{n} \mu_i^*(N_{\{i\}})N_i - \sum_{i=1}^{n} \int_{-\infty}^{\mu_i^*(N_{\{i\}})} N_i d\mu_i(N_{\{i\}}) \quad (7)$$

where μ_i^* is the specified chemical potential of each of the components. This means that we obtain ΔF without needing to know the hydrostatic pressure at zero loading. The right-hand side of this expression can be obtained from GCMC simulations, in which one specifies the chemical potential of the guest components and measures the number of the guest molecules. Because the Helmholtz energy is a state function, the integration in eq 7 can be performed along any path as long as the starting and final points are the same. However, the form above is convenient for integration because at low loadings the slope of the function $N_i(\mu_i)$ approaches zero. The integration in eq 7 over the chemical potential of one component is performed by keeping the chemical potentials of all other components fixed. For a two-component system, it is convenient to perform this integration first along the path of $\mu_2 = -\infty$ from $\mu_1 = -\infty$ to $\mu_1 = \mu_1^*$ and then along the path $\mu_1 = \mu_1^*$ from $\mu_2 = -\infty$ to $\mu_2 = \mu_2^*$.

The chemical potential of the ith component directly follows from its fugacity f_i[16,17]

$$\mu_i = -k_B T \ln(RTq_i/f_i) \quad (8)$$

Here $q_i \equiv Z_{int,i}/(N_A\Lambda_i^3)$, where $Z_{int,i}$ is the partition function for internal degrees of freedom. If the molecules are rigid (which is the case for our simulations, see Section 3), then $Z_{int,i}$ has contributions only from rotation of the molecule. At high temperature, $Z_{int,i} = T/T_r$, where T_r is the characteristic temperature of the rotational degrees of freedom. Furthermore, $\Lambda_i \equiv hN_A/(2\pi M_i RT)^{1/2}$ is the thermal de Broglie wavelength of component i, M_i is the molar mass, and h, N_A, R, k_B are Planck's constant, Avogadro's number, the universal gas constant, and Boltzmann's constant, respectively.

2.2. Heat of Encapsulation. The heat of encapsulation of gas(es) into the hydrate at constant volume is defined as the internal energy change of reaction 1 at constant volume. From the internal energy of reaction 1, we define the partial molar energy for encapsulation of a component i

$$\Delta_r U_i = \left(\frac{\partial \Delta_r U}{\partial N_i}\right)_{N_j,V,T} = \left(\frac{\partial (U^h - U^g)}{\partial N_i}\right)_{N_j,V,T} \quad (9)$$

where U^h is the internal energy of the gas and water in the hydrate phase and U^g is the corresponding value for the internal energy of the gas and water in the gas phase. For a guest molecule, both energies have constant contributions from the translational energy, $(s_i/2)k_BTN_i$, where s_i is the number of degrees of freedom of the component, and these contributions cancel in the difference.[18] We will consider rigid molecules, which is the case for simulations performed (see below). This would mean that any contributions to the internal energy due to the internal degrees of freedom of the molecules cancel in eq 9 as well, as they are the same in the gas phase and in the hydrate phase. The remaining contribution is due to the difference between the configurational parts of the internal energy caused by intermolecular interactions, which are denoted by U_c^h and U_c^g. In the literature, it is common to consider the gas to be ideal so that it acts as a reference state to the guest components; therefore, $U_c^g = 0$. Furthermore, it is common to define the partial molar heat of encapsulation as the partial molar enthalpy difference rather than the partial molar internal energy difference.[14,18] For ideal gas, this adds the constant RT to the partial molar internal energy difference. This defines the partial molar heat of encapsulation q_i as

$$-q_i = \left(\frac{\partial U_c^h}{\partial N_i}\right)_{N_j,T,V} - RT \quad (10)$$

In this study, we are interested only in the hydrate phase. The quantity $-q_i$ defined by eq 10 is then a property of a hydrate phase with reference to an ideal gas phase. This is typical in the simulation community and conforms with the discussion in Section 2.1 to describe the hydrate phase only.[14] We shall use eq 10 for hydrates filled with single components and calculate the molar heat of encapsulation of CH_4 and CO_2.

The derivative of the internal energy of the hydrate with respect to the number of guest molecules can be calculated in a number of ways.[14] In GCMC simulations, one calculates the molar heat of encapsulation 10 from the fluctuations of the thermodynamic quantities as[15,18]

$$q = RT - \frac{\langle \delta U_c^h \delta N \rangle}{\langle \delta N \delta N \rangle} \quad (11)$$

where $\langle \delta X\, \delta Y \rangle \equiv \langle XY \rangle - \langle X \rangle \langle Y \rangle$ and $\langle\rangle$ denotes an ensemble average in the grand-canonical ensemble.

3. SIMULATION DETAILS

We perform GCMC (μVT) simulations of CH_4 and CO_2 in a 2 × 2 × 2 unit cell of sI hydrate, which has 64 cages. The cubic unit cell has a lattice parameter of 12.03 Å.[11] The system becomes equilibrated rather quickly, typically after 300−500 cycles. The number of cycles, during which the statistics for averaging is accumulated, was varying from 500 to 500 000 to achieve the desired accuracy. The number of MC moves per cycle is equal to the number of particles of each component in the system, with a minimum of 20.

In GCMC simulations, one specifies the chemical potential of each of the components and calculates the average number of particles that corresponds to this chemical potential.[19] For pure components, fugacities and pressures can be converted using the equation of state for the system. Here we used the Peng−Robinson EOS, which can describe the pressure of the gas phase well far from the critical point. PR-EOS was found to be rather accurate for the description of both experimental data[20] and interaction potentials[21] for CO_2 and CH_4. The values of the critical temperature, critical pressure, and the acentric factor required for PR-EOS used in this potentials are, respectively, 304.1282 and 190.564 K, 7 377 300.0 and 4 599 200.0 Pa, and 0.22394 and 0.01142 for CO_2 and CH_4.[21] For

dx.doi.org/10.1021/jp2119586 | J. Phys. Chem. B 2012, 116, 3745−3753

mixtures, we applied the Lewis-Randall rule[17] to convert pressures and fugacities from pure phase values to mixture values. The methane−carbon dioxide mixture reveals the behavior of the regular solution,[22] but it is common to approximate it as an ideal solution[23] because the excess enthalpy is small.

In the semigrand canonical MC simulations, we specify N_w and f_i or μ_i, i = 1...n, and find the loading of the guest components N_i and accordingly the Helmholtz energy of the gas mixture in the hydrate; see eq 7. In our GCMC simulations, the molecules were allowed to change their position and orientation. They were also subjected to Regrow, Swap, and Identity change[24] MC moves. Furthermore, a series of NVT simulations was performed to analyze the distribution of molecules between the cages. In NVT simulations, one specifies the total number of guest molecules, whereas they are allowed to distribute among the cages: the guest molecules were allowed to change their position and orientation.

The oxygen positions of water molecules were taken from crystallographic data.[11] The orientation of hydrogen atoms was chosen random in accordance with the Bernal−Fowler rule.[25] Initially all hydrogen atoms were assigned randomly to each of four sites of the water molecule (two sites from the hydrogens and two sites for the hydrogen bonds to the neighboring molecule). Then, a short Monte Carlo procedure was performed to displace the hydrogen atoms between the sites randomly to satisfy two conditions: (i) each oxygen atom has only two hydrogen atoms and (ii) there is only one hydrogen atom between each two oxygen atoms. The third requirement, that the number of the hydrogen atoms of the corresponding Wyckoff type is given, was satisfied automatically after the above procedure.

We used the TIP5PEw model of water.[26] We performed simulations with both immobile and mobile water molecules (the water framework is then called rigid and flexible, respectively), so in the latter case they were allowed to change their position and orientation. During the simulations, we found that behavior of the rigid framework and the flexible framework is similar, whereas the fluctuations in the number of the guest molecules were larger for the case of the flexible network. In the analysis of the results, we therefore present the data for a rigid water framework. The description of the guest molecules was taken from the TraPPE force field.[27] We use the LJ interaction potential, truncated and shifted to zero at 12 Å. The parameters of the potential are given in Table 1, and the parameters of atoms are given in Table 2. Ewald summation was used with relative precision 10^{-6} and alpha convergence parameter 0.265058.

Table 1. Parameters of LJ Interaction Potential between C and O Atoms in CH_4, CO_2, and H_2O Molecules[21]

atomic pairs	$\varepsilon/(k_B\mathrm{K})$	σ/Å
C_{CH_4}−C_{CH_4}	158.50000000	3.72000000
C_{CH_4}−C_{CO_2}	68.87985475	3.23237650
C_{CH_4}−O_{CO_2}	116.52842617	3.36866350
C_{CH_4}−O_{H_2O}	119.11459189	3.40850000
C_{CO_2}−C_{CO_2}	28.12900000	2.76000000
C_{CO_2}−O_{CO_2}	47.59000000	2.89000000
C_{CO_2}−O_{H_2O}	51.76401128	2.92087650
O_{CO_2}−O_{CO_2}	80.50700000	3.03300000
O_{CO_2}−O_{H_2O}	87.57246641	3.05716350
O_{H_2O}−O_{H_2O}	89.51600000	3.09700000

Table 2. Mass, m, Charge, q, and Bond Length, r, of Atoms in CH_4, CO_2, and H_2O Molecules[21] [a]

atoms	$m/1.6605402 \times 10^{-27}$ kg	$q/1.60217733 \times 10^{-19}$ C	r/Å
C_{CH_4}	16.04246	0.0	1.00
C_{CO_2}	12.0	0.6512	0.720
O_{CO_2}	15.9994	−0.3256	0.68
O_{H_2O}	15.9994	0.0	0.5
H_{H_2O}	1.008	0.241	1.00
L_{H_2O}	0.0	−0.241	1.00

[a] Atoms i and j are considered to be "bonded" if the distance between the atoms is smaller then $0.56 + r_I + r_j$.

We performed simulations for the temperature range 278−328 K. The occupancy isotherms were qualitatively the same for all temperatures in this range. We therefore focused on the temperature of 278 K. The pressure and fugacities varied in the range between 10^4 and 10^9 Pa in these simulations.

4. RESULTS OF THE SIMULATIONS

4.1. Single-Component Occupancy Isotherms. The single-component occupancy isotherms for CO_2 and CH_4 at 278 K are shown in Figure 1. We see how the hydrate loading, N, varies with applied pressure, p, on a sI unit cell with eight cages. The pressure axis is given on a logarithmic scale. For a

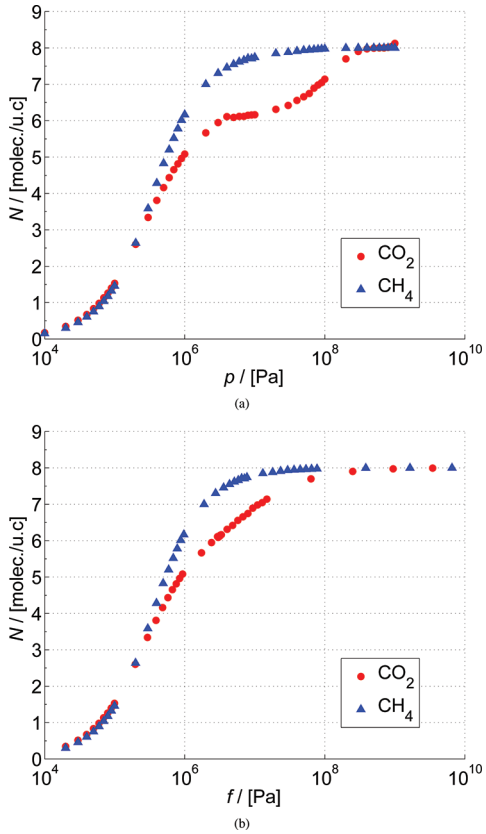

Figure 1. Number of guest molecules per unit cell of a sI hydrate as a function of the applied pressure (a) and fugacity (b) as computed by GCMC simulations at T = 278 K.

dx.doi.org/10.1021/jp2119586 | J. Phys. Chem. B 2012, 116, 3745−3753

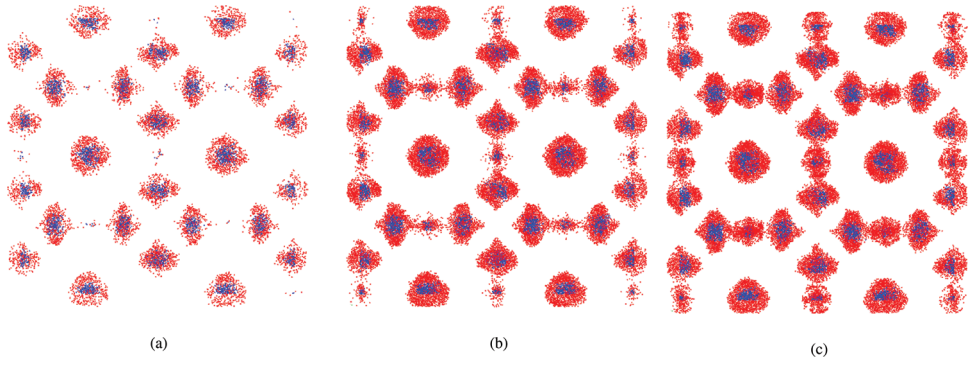

Figure 2. Distribution of CO_2 molecules in the clathrate cages of a box with 2 × 2 × 2 unit cells of sI hydrate (64 cages) at various loading: (a) N = 11 molecules, (b) N = 48 molecules, and (c) N = 66 molecules. Carbon atoms are blue, oxygen atoms are red, and water molecules are not displayed for clarity.

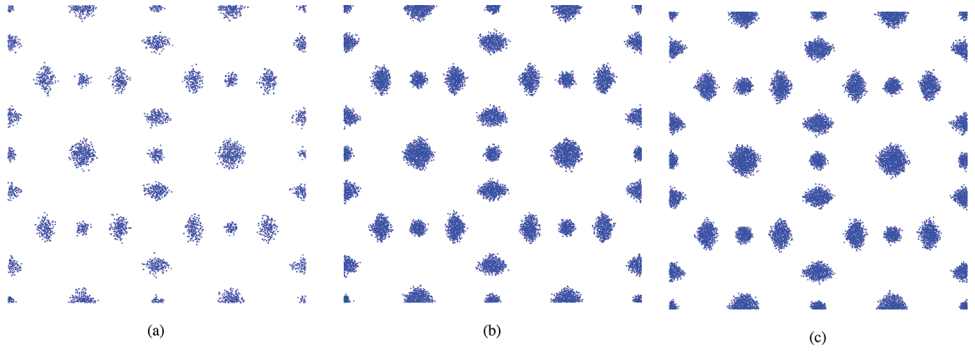

Figure 3. Distribution of CH_4 molecules in the clathrate cages of a box with 2 × 2 × 2 unit cells of sI hydrate (64 cages) at various loading: (a) N = 11 molecules, (b) N = 48 molecules, and (c) N = 66 molecules. CH_4 molecules are colored blue, and water molecules are not displayed for clarity.

hydrate with the rigid water framework the error bar is less than the size of the symbol. The occupancy isotherms of CO_2 and CH_4 for the case of the flexible water framework are similar (not shown).

At first sight, the occupancy isotherms in Figure 1a may look like Langmuir adsorption isotherms; however, the fitting of the one- or two-site profiles to such isotherms is not satisfactory: it deviates from the ideal one. Still, the CO_2 isotherm reveals a two-site adsorption behavior. This can be explained by the structure of sI clathrate. A unit cell of an sI hydrate has six large and two small cages. Being a relatively large molecule, CO_2 tends to occupy large cages first. (The diameter of CO_2 molecule is 5.12 Å, whereas the average cage diameters of large and small cages are 7.9 Å and 8.66 Å^2.) Small cages start to be filled only after the large cages have been occupied.

Figure 2 shows the distribution of CO_2 molecules between several cages, obtained from a NVT simulation. The positions of these molecules from 500 snapshots were combined and plotted on a single figure. When the loading of CO_2 is small (N = 11), the loading of the large cages is much larger than the population of small cages. At intermediate loading (N = 48), which corresponds to the plateau in the CO_2 occupancy isotherm, some small cages start to be filled, whereas the other small cages remain almost unoccupied. Finally, at high loading (N = 66), all cages are occupied uniformly. The cell with 2 × 2 × 2 units of sI clathrate has 64 cages. Having 66 molecules encaged into clathrate means that some cages contain two CO_2 molecules. This happens at large pressures only.

The CH_4 isotherm, reveals a one-site adsorption behavior. The reason for this is that CH_4 molecules are rather small (diameter of CH_4 molecule is 4.36 Å^2) and have almost no preference between large and small cages. However, the observation that there are two types of cages is relevant for the CH_4 distribution: otherwise the occupancy isotherm would be a perfect single-site Langmuir curve. The typical distribution of CH_4 molecules is shown in Figure 3. The snapshots were obtained in the same way as those in Figure 2. This Figure shows that CH_4 fills the cages uniformly, showing almost no preference to large or small cages, in contrast with the behavior of CO_2.

4.2. Heats of Encapsulation. Figure 4 shows the partial molar heats of encapsulation, eq 11, of the single component hydrates as a function of loading obtained from GCMC simulations. At high loading ($N \approx 7$ molecules per unit cell),

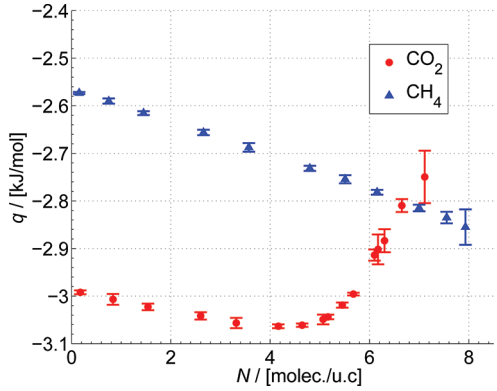

Figure 4. Partial molar heat of encapsulation of a single-component hydrate as computed by GCMC simulations at 278 K as a function of the loading of a single-component hydrate.

dx.doi.org/10.1021/jp2119586 | J. Phys. Chem. B 2012, 116, 3745−3753

the calculated value of the partial molar heat of encapsulation starts to fluctuate. This is expected for GCMC simulations because in the dense phase, which is realized at high loadings, the fraction of accepted trial MC moves is quite low. This means that we shall trust the results at small and moderate loadings only (not more than six to seven guest molecules per unit cell).

We see in Figure 4 that the partial molar heat of encapsulation of CH_4 decreases almost linearly with the loading over the whole range of loadings. The single-site occupancy isotherm shown in Figure 1a for methane can thus be explained by Figure 4 alone. In contrast, for carbon dioxide, one can distinguish the two regions for the partial molar heat of encapsulation of CO_2. At small loadings the partial molar heat of encapsulation decreases when loading increases, similar to that for CH_4. This correspond to low pressures, and mostly the large cages of the hydrate are being filled in. At moderate loadings the partial molar heat of encapsulation has a tendency to increase, however. This corresponds to the filling of the small cages of the hydrate. Because the CO_2 molecules prefer not to be in the small cages, more and more energy is required to get them into the hydrate at high pressures. The shape of the curve in Figure 4 can explain the occupancy isotherm for CO_2 shown in Figure 1a. Indeed, the profiles presented in Figure 4 at small loadings are not exactly linear, which implies that the occupancy isotherm cannot be described by a Langmuir isotherm.

As one can see from Figure 4, the profile of CO_2 heat of encapsulation changes direction not at $N = 6$ molecules per unit cell, which corresponds to the complete filling of the large cages. The minimum is when only four to five cages are occupied. This may be explained by the strong interactions of large asymmetric CO_2 molecule with water cages.[5] The partial molar heat of encapsulation of CO_2 is lower than the one of CH_4 over the whole range of loadings that can be trusted. This supports the preferential filling of the large cages by CO_2 molecules.

4.3. Mixture Occupancy Isotherms. Isotherms for hydrates loaded with mixtures of CO_2 and CH_4 are shown in Figure 5. This Figure shows the CO_2 mole fraction in the hydrate as a function of the gas pressure and the corresponding CO_2 mole fraction in the gas phase. One can identify two regions in the figure, with the pressure above ~10^7 Pa and below 10^7 Pa. As one can see from Figure 1a, this is approximately the pressure where the occupancy isotherm of CO_2 reaches the plateau. In both regions, the molar content of CO_2 in the hydrate increases gradually when the content of CO_2 in the gas phase increases. When the pressure is below 10^7 Pa, the CO_2 molecules fill the large cages, whereas the CH_4 molecules fill both the small and the large cages. Therefore, there is no preference between large and small cages. Therefore, the mixture composition in the hydrate is approximately the same as that in the gas phase over the whole range of compositions; see Figure 6. At ~10^7 Pa, the large cages are all filled, and only small cages are available. CO_2 molecules cannot compete with CH_4 molecules for these cages because the former ones are larger than the latter ones. It is mostly CH_4 molecules that occupy the small cages in the mixture; see Figure 6.

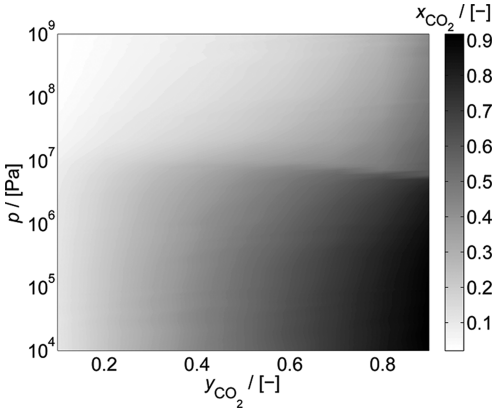

Figure 5. Mole fraction of CO_2 (darkness) in the CO_2 + CH_4 gas mixture in the hydrate at 278 K computed by GCMC simulations as a function of the gas pressure and the mol fraction of CO_2 in the gas described by the Peng–Robinson equation of state.

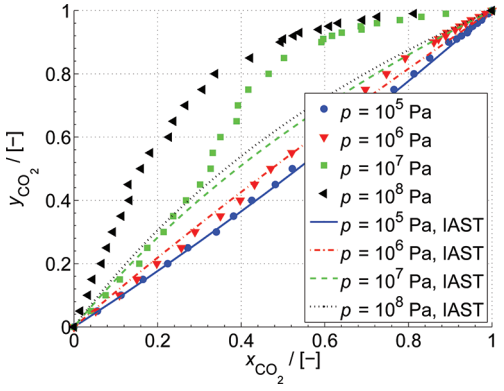

Figure 6. Mole fraction of CO_2 in the gas mixture, y, as a function of its mole fraction in the hydrate, x, at 278 K for various gas pressures, as computed by GCMC simulations and compared with the predictions of ideal adsorption theory (IAST).

Figure 6 compares the results of the mixture loading with ideal adsorption solution theory (IAST).[28] The concept of ideal solution for the adsorbed components is analogous to the Raoult's law for vapor–liquid equilibrium. It holds well for mixtures of similar components, which are adsorbed on similar sites. For segregated systems (when one component adsorbs on one type of sites while the other component adsorbs on the other adsorption sites), it is known that it does not work.[29,30] Furthermore, this theory can be directly applied to hydrate systems. As one can see from Figure 6, the mixture can be considered ideal at small pressures, which are below the pressure when the CO_2 loading reaches the plateau. At these pressures, the CO_2 and CH_4 molecules occupy the large cages equally likely. Even though the CH_4 and CO_2 molecules are different, the large cages are so large that they show no preference to the components they would encage. At pressures larger than 10^7 Pa, we observe preferential occupancy for CH_4 molecules, so the mixture cannot be considered as being ideal. At these pressures, the small cages are filled, so it is natural that they prefer small CH_4 molecules rather than large CO_2 molecules. It becomes clear that at high pressures that IAST does not hold.

We next consider the dependence of loading on the fugacity of each of the component, which is shown in Figure 7. We see that the loading of each of the component increases proportionally to its fugacity. Furthermore, the increase in the fugacity of one of the components complicates the occupancy

dx.doi.org/10.1021/jp2119586 | J. Phys. Chem. B 2012, 116, 3745–3753

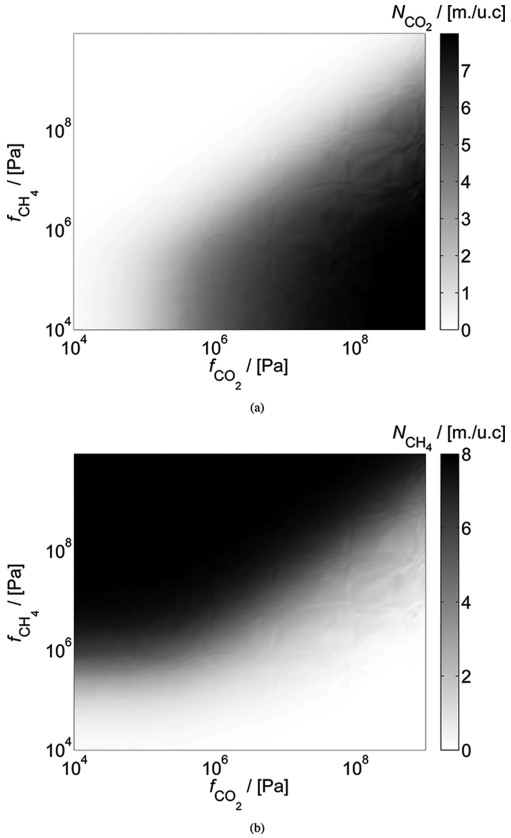

Figure 7. Loading per unit cell (darkness) of each of the component in the CO_2 + CH_4 gas mixture in the hydrate at 278 K as a function of the fugacity of each of the component: (a) loading of CO_2 and (b) loading of CH_4.

of the other component and vice versa. This behavior is consistent with the occupancy isotherms in Figure 1b.

4.4. Helmholtz Energy of the Pure Gases and Gas Mixtures in Hydrates. We first report the Helmholtz energy for the single-component hydrates. Figure 8 shows this Helmholtz energy for CO_2 and CH_4 hydrates. One can see that the more molecules encaged, the lower the Helmholtz energy per mole. This means that the hydrate is becoming relatively more stable as the number of molecules increases. This is well-known,[2] because empty cavities are not stable and guest molecules are required to stabilize them. Furthermore,

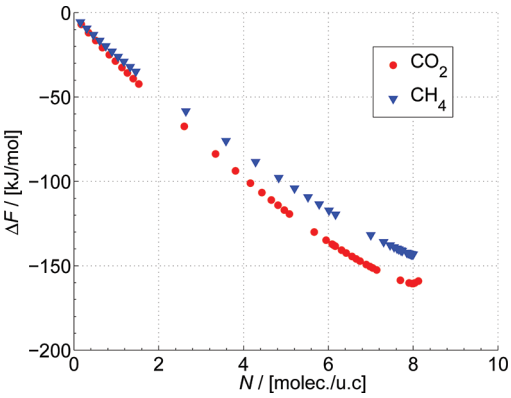

Figure 8. Helmholtz energy of a single component hydrate at 278 K as a function of the hydrate loading per unit cell.

one can see that the Helmholtz energy for the CO_2 hydrate is lower than that of the CH_4 hydrate over the whole range of loadings. This indicates that the CO_2 hydrate is more stable than the CH_4 hydrate.

We next consider the Helmholtz energy of the gas mixtures in the hydrate. Figure 9 shows how the Helmholtz energy depends on the fugacities of each of the components. We see

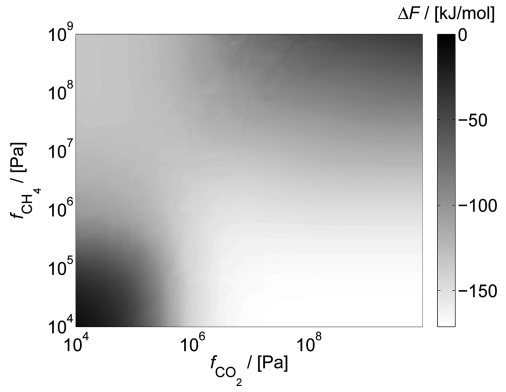

Figure 9. Helmholtz energy difference (darkness) as computed by eq 7 of the CO_2 + CH_4 gas mixture in the hydrate at 278 K as a function of the fugacity of each of the component.

that there is a certain region where this energy is lowest, so the hydrate with gas mixture would be more stable at these compositions. At low fugacities, there are not that many molecules encaged, which means that many cages are empty. This makes the gas hydrate structure less stable, which explains the dark region in Figure 9 in the bottom-left corner. If both fugacities are high, then both CO_2 and CH_4 molecules prefer to occupy the cages. Competition for an available cage makes the hydrate structure less stable as well. This is indicated by the dark region in Figure 9 in the top-right corner. Finally, if only one of the two fugacities is large, whereas the other is low, then only the high-fugacity molecules tend to fill the cages and the hydrate structure becomes relatively more stable.

These considerations of stability are not conclusive, however. As explained in the Introduction, a more complete set of thermodynamic data is needed to evaluate the possibility of hydrate formation. Namely, the values of the Helmholtz energy of different phases, which can be formed of CH_4, CO_2, and water, are required. We shall return to this point in our next work.

4.5. Possible Thermodynamic Path for Converting Methane Hydrate to Carbon Dioxide Hydrate. It is interesting to plot Figure 9 on a p–y scale, where p is the gas pressure, the components' chemical potentials of which are identical to the ones in the hydrate and y is the mole fraction of CO_2 in the gas phase. The distribution of the Helmholtz energy of the hydrate with gas mixture for this case is shown in Figure 10a. We see that the hydrate is more stable at high pressures (i.e., at high loadings) if pure gas is being encaged. In contrast, if we have a mixture, then the highest stability is achieved at moderate pressures.

Figure 10a shows that there is a region in the pressure–composition diagram that connects a relatively stable methane hydrate with a relatively stable carbon dioxide hydrate. Whereas at low and high pressures a hydrate with gas mixture is less stable, it is almost as stable as either single-component hydrate at moderate pressures. This is very promising because we want

dx.doi.org/10.1021/jp2119586 | J. Phys. Chem. B 2012, 116, 3745–3753

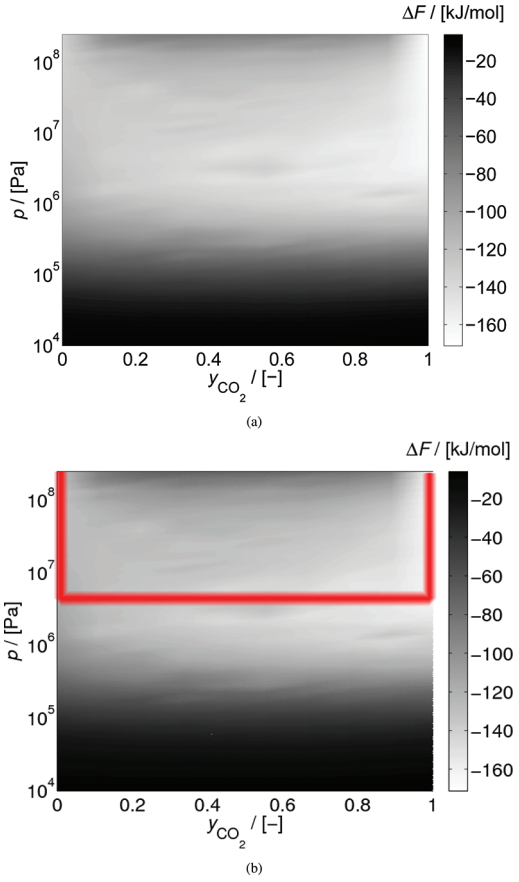

Figure 10. (a) Helmholtz energy difference (darkness) as computed by eq 7 of the CO_2 + CH_4 gas mixture in the hydrate at 278 K as a function of the gas pressure and mol fraction of CO_2 in the gas phase. (b) Path on the diagram to convert a pure CH_4 hydrate to a pure CO_2 hydrate.

to find a path on a phase diagram to convert a pure CH_4 hydrate into a pure CO_2 hydrate without destroying its structure. In a pursuit of this path, it will therefore be interesting to focus on the lightest-colored region on the diagram. In Figure 10b, this path is drawn schematically. To follow this path implies that one does not meet any energy barrier: the value of ΔF along it is almost everywhere constant. In contrast, going from pure CH_4 hydrate to pure CO_2 hydrate at constant pressure around 10^8 to 10^9 Pa requires crossing an energy barrier of 50−100 kJ per mol of unit cell.

We see that this path goes through a region where a mixture of CH_4 and CO_2 is encaged into a hydrate. Namely, one has first to decrease the pressure of pure CH_4 hydrate to $\sim 10^7$ Pa. At this pressure, there is enough space in the large cages for CO_2 molecules to enter. Next, one has to increase the content of CO_2 in the surrounding fluid. This would lead to the filling of the large cages with CO_2 molecules, whereas the CH_4 molecules will be expelled from the hydrate. When there is no CH_4 in the mixture, the small cages are empty at the pressure 10^7 Pa, and this is the time to start filling them in with the CO_2 molecules. This is the last part of our path, which ends up with a pure CO_2 hydrate.

The cage's windows are small, so neither CH_4 nor CO_2 can physically go through them. It is not possible for a gas molecules to travel between cages of a completely ideal structure. The process above can therefore not be realized as a diffusion process. However, it has been shown that the gas molecules can travel between the cages if some of the water molecules are missing.[31] We still call such defect structure undestroyed, in contrast with a situation, when the whole hydrate melts down to a water solution. Furthermore, one can think of the exchange via growth of the hydrate[32] on one side of a volume element and depletion on the other side. Experimental studies[33] show that the exchange of methane with carbon dioxide in the hydrates is not only favorable from the thermodynamic point of view but also from kinetic perspectives. This all looks promising in the view of the potential use of the suggested thermodynamic path. Finally, it is important to remember that the above procedure is possible if along the path the hydrate is more stable than the possible liquid mixture under the same conditions. These factors are important for a practical realization of the path and will be examined in more detail in a paper to come.

5. CONCLUSIONS

In this Article, we studied the thermodynamic properties of an sI hydrate filled with CO_2, CH_4, and the mixture of those. By performing GCMC simulations, we obtained occupancy isotherms for single components and gas mixtures, partial molar heats of encapsulation of single components, and the Helmholtz energy of a hydrate with the gas mixture referred to an empty hydrate.

The results show that the state of the hydrate is determined by the relation between the size of the clathrate cages and the guest molecules. The small methane molecules can easily fill both the large and the small cages, whereas the larger molecules of carbon dioxide prefer the large cages. This determines the two regions of the hydrate state with various loading.

At a small pressure, the CO_2 molecules tend to fill the large cages only. Then, the small cages are filled. Whereas the hydrate is still becoming more stable (the Helmholtz energy is decreasing), the relative increase in stability becomes smaller. The methane occupancy reveals almost no preference to cage type, so the partial molar heat of encapsulation is always decreasing, which means that every new molecule is more welcome than the previous one. The Helmholtz energy is always decreasing, which means that the fully occupied hydrate is the most stable one compared with a partially filled hydrate.

The single-component occupancy behavior determines the regime of mixture occupancy. The guest mixture may be regarded as ideal but only when the large cages are being filled. At this point, there is almost no difference between the behavior of CO_2 and CH_4 molecules. In contrast, when small cages start to be filled, the hydrate with gas mixture reveals strong preference to CH_4 occupancy.

Finally, Figure 10b obtained for the Helmholtz energy of the gas mixture in hydrate is promising. It may suggest a way to convert CH_4 hydrates, which are excessively available at the sea bottoms, to CO_2 hydrates. From the kinetic point of view, it may be complicated to perform an exchange of molecules in a hydrate because unlike zeolites a hydrate does not have empty channels for molecules to go in. In practice, the exchange could be performed in a distorted clathrate structure.[31] The existence of such a path must presently be seen as qualitative, as we are lacking information on the thermodynamic properties of the other phases, which can be in equilibrium with the hydrate phase, cf. eq 1. Our further efforts are now directed into calculating the phase diagram and the remaining thermodynamic data.

dx.doi.org/10.1021/jp2119586 | J. Phys. Chem. B 2012, 116, 3745−3753

AUTHOR INFORMATION

Corresponding Author

*E-mail: kirill.glavatskiy@nt.ntnu.no.

Notes

The authors declare no competing financial interest.

ACKNOWLEDGMENTS

We would like to thank Juan-Manuel Castillo Sanches for help with simulations, Bjørn Kvamme for fruitful discussions, and J. H. van der Waals for useful comments. We are also grateful to the VISTA grant no. 6343.

REFERENCES

(1) Sloan, E. D. *Nature* **2003**, *426*, 353−363.
(2) Sloan, E. D. *Clathrate Hydrates of Natural Gases*, 2nd ed.; Marcel Dekker, Inc.: New York, 1998.
(3) Tegze, G.; Gránásy, L.; Kvamme, B. *Phys. Chem. Chem. Phys.* **2007**, *9*, 3104−3111.
(4) Baldwin, B. A.; Stevens, J.; J.Howard, J.; Graue, A.; Kvamme, B.; Aspens, E.; Ersland, G.; Husebø, J.; Zornes, D. R. *Magn. Reson. Imaging* **2009**, *27*, 720−726.
(5) Kvamme, B.; Graue, A.; Buanes, T.; Kuznetsova, T.; Ersland, G. *Int. J. Greenhouse Gas Control* **2007**, *1*, 236−246.
(6) Geng, C.-Y.; Wen, H.; Zhou, H. *J. Phys. Chem. A* **2009**, *113*, 5463−5469.
(7) Papadimitriou, N. I.; Tsimpanogiannis, I. N.; Papaioannou, A.; Stubos, A. K. *Mol. Simul.* **2008**, *34*, 1311−1320.
(8) Katsumasa, K.; Koga, K.; Tanaka, H. *J. Chem. Phys.* **2007**, *127*, 044509.
(9) Wierzchowski, S. J.; Monson, P. A. *J. Phys. Chem. B* **2007**, *111*, 7274−7282.
(10) Wierzchowski, S. J.; Monson, P. A. *Ind. Eng. Chem. Res.* **2006**, *45*, 424−431.
(11) McMullan, R. K.; Jeffrey, G. A. *J. Chem. Phys.* **1965**, *42*, 2725−2732.
(12) Castillo, J. M.; Dubbeldam, D.; Vlugt, T. J. H.; Smit, B.; Calero, S. *Mol. Simul.* **2009**, *35*, 1067−1076.
(13) Frenkel, D.; Ladd, A. J. C. *J. Chem. Phys.* **1984**, *81*, 3188−3193.
(14) Vlugt, T. J. H.; García-Pérez, E.; Dubbeldam, D.; Ban, S.; Calero, S. *J. Chem. Theory Comput.* **2008**, *4*, 1107−1118.
(15) Karavias, F.; Myers, A. *Langmuir* **1991**, *7*, 3118−3126.
(16) Landau, L. D.; Lifshitz, E. M. *Statistical Physics*, 3rd ed.; Course of Theoretical Physics *5*; Pergamon Press: London, 1986.
(17) Moran, M. J.; Shapiro, H. N. *Fundamentals of Engineering Thermodynamics*, 5th ed.; John Wiley & Sons, Inc.: New York, 2006.
(18) Nicholson, D.; Parsonage, N. *Computer Simulations and the Statistical Mechanics of Adsorption*, 2nd ed.; Academic Press: New York, 1982.
(19) Frenkel, D.; Smit, B. *Understanding Molecular Simulation. From Algorithms to Applications*, 2nd ed.; Academic Press: New York, 2002.
(20) Peng, D.-Y.; Robinson, D. B. *Ind. Eng. Chem. Fundam.* **1976**, *15*, 59−64.
(21) García-Pérez, E.; Parra, J. B.; Ania, C. O.; Garciá-Sánchez, A.; van Baten, J. M.; Krishna, R.; Dubbeldam, D.; Calero, S. *Adsorption* **2007**, *13*, 469−476.
(22) Barry, A. O.; Kaliaguine, S. C.; Ramalho, R. S. *J. Chem. Eng. Data* **1982**, *27*, 258−264.
(23) Arai, Y.; Kaminishi, G.-I.; Saito, S. *J. Chem. Eng. Jpn.* **1971**, *4*, 113−122.
(24) Martin, M. G.; Siepmann, J. I. *J. Am. Chem. Soc.* **1997**, *119*, 8921−8924.
(25) Bernal, J. D.; Fowler, R. H. *J. Chem. Phys.* **1933**, *1*, 515−548.
(26) Rick, S. W. *J. Chem. Phys.* **2004**, *120*, 6085−6093.
(27) Potoff, J. J.; Siepmann, J. I. *AIChE J.* **2001**, *47*, 1676−1682.
(28) Myers, A. L.; Prausnitz, J. M. *AIChE J.* **1965**, *11*, 121−127.
(29) Krishna, R.; Paschek, D. *Phys. Chem. Chem. Phys.* **2001**, *3*, 453−462.
(30) Murthi, M.; Snurr, R. Q. *Langmuir* **2004**, *20*, 2489−2497.
(31) Peters, B.; Zimmermann, N. E. R.; Beckham, G. T.; Tester, J. W.; Trout, B. L. *J. Am. Chem. Soc.* **2008**, *130*, 17342−17350.
(32) Liang, S.; Kusalik, P. G. *Chem. Phys. Lett.* **2010**, *494*, 123−133.
(33) He, Y.; Rudolph, E. S. J.; Zitha, P.; Golombok, M. *Fuel* **2011**, *90*, 272−279.